Aust. J. Phys., 1995, **48**, 557–69

Velocity Distribution Functions and Transport Coefficients of Electron Swarms in Gases in the Presence of Crossed Electric and Magnetic Fields*

K. F. Ness

Physics Department, James Cook University,
Townsville, Qld 4811, Australia.

Abstract

A multi-term solution of the Boltzmann equation is used to calculate the spatially homogeneous velocity distribution function of a dilute swarm of electrons moving through a background of denser neutral molecules in the presence of crossed electric and magnetic fields. As an example, electron motion in methane is considered.

1. Introduction

Despite a long history of investigation (Allis 1955; Huxley and Crompton 1974; Heylen 1980) many aspects of charged-particle transport through neutral gases in the presence of both electric and magnetic fields remains unexplored. This is true from both an experimental and theoretical perspective, and is in part due to the practical and theoretical problems that arise when the magnetic field is included with no desired loss of precision in either measurement or calculation.

In recent years interest in charged-particle transport through neutral gases under the conditions of crossed electric and magnetic fields has revived. This interest was in part motivated by the desire to understand the physics underlying the operation of wirechambers in which the geometry of crossed electric and magnetic play an important role (Heintze 1978; 1982). Of more fundamental interest is the possibility of using data obtained from $\boldsymbol{E}\times\boldsymbol{B}$ experiments in the swarm derivation of electron–molecule scattering cross sections (Schmidt 1993; Schmidt *et al.* 1994). In order to achieve this, a general, accurate theory (at least as accurate as experiment) is required. Such a theory, $\boldsymbol{E}\times\boldsymbol{B}$ based on the spherical-harmonic decomposition of the Boltzmann equation, has been published by the author (Ness 1993). In that paper the general formalism was given for solving the Boltzmann equation for reacting charged-particle swarms in neutral gases in the presence of an electric and magnetic field set at some arbitrary angle to each other. In subsequent papers (Ness 1994; Ness and Robson 1994) a numerical solution for the case of non-reacting swarms in perpendicular fields was given for both model and real gases; transport coefficients and other average properties were presented. The present work is part of an on-going theoretical investigation into charged-particle transport through gases in the presence of

* Refereed paper based on a presentation to the Third Japan–Australia Workshop on Gaseous Electronics and Its Applications, held at Yeppoon, Queensland, in July 1994.

0004-9506/95/030557$05.00

electric and magnetic fields. Here we focus on the velocity distribution function rather than transport coefficients. In the following section a brief outline of the theory is given; for more detailed theory the reader is referred to Ness (1993, 1994).

2. Theory

Theoretically, all relevant information about the swarm can be obtained from the phase space distribution function $f(\boldsymbol{r}, \boldsymbol{c}, t)$. Under the present conditions $f(\boldsymbol{r}, \boldsymbol{c}, t)$ is the solution of the Boltzmann equation

$$\left[\partial_t + \boldsymbol{c}\cdot\nabla + \frac{e}{m}(\boldsymbol{E} + \boldsymbol{c}\times\boldsymbol{B})\cdot\partial_c + J\right] f = 0, \tag{1}$$

where all symbols have their usual meaning (Ness 1993, 1994). In the present approach equation (1) is solved by decomposing $f(\boldsymbol{r}, \boldsymbol{c}, t)$ in terms of spherical harmonics in velocity space and powers of the gradient operation acting on the number density $n(\boldsymbol{r}, t)$ in real space, i.e.

$$f(\boldsymbol{r}, \boldsymbol{c}, t) = \sum_{l=0}^{\infty}\sum_{m=-l}^{l}\sum_{s=0}^{\infty}\sum_{\lambda=0}^{s}\sum_{\mu=-\lambda}^{\lambda} f(lm\,|\,s\lambda\mu) Y_m^{[l]}(\hat{\boldsymbol{c}}) G^{(s\lambda)} n(\boldsymbol{r}, t). \tag{2}$$

Here $Y_m^{[l]}(\hat{\boldsymbol{c}})$ denotes the spherical harmonics which are functions of the polar angles $\hat{\boldsymbol{c}} \equiv \theta, \phi$ of $\boldsymbol{c}$, and $G_\mu^{(s\lambda)}$ denotes the sth application of the gradient operator in irreducible tensor notation.

Substitution of equation (2) into (1) and carrying out the necessary operations (Ness 1993) reduces (1) to an infinite set of coupled one-dimensional integro-differential equations for the functions of speed $f(lm\,|\,s\lambda\mu)$. This set of equations is finally reduced to a matrix equation by expanding the speed dependence of the $f(lm\,|\,s\lambda\mu)$ in terms of Sonine polynomials about a Maxwellian distribution at some base temperature T_b, i.e.

$$f(lm\,|\,s\lambda\mu) = \bar{w}(\alpha, c)\sum_{\nu=0}^{\infty} F(\nu lm\,|\,s\lambda\mu) R_{\nu l}(\alpha c), \tag{3}$$

where $\alpha^2 = m/kT_b$, $\bar{w}(\alpha, c)$ is a Maxwellian,

$$R_{\nu l}(\alpha c) \;=\; N_{\nu l}\left[\frac{\alpha c}{\sqrt{2}}\right]^l S_{l+\frac{1}{2}}^{(\nu)}(\alpha^2 c^2/2)\,, \tag{4}$$

$$N_{\nu l}^2 \;=\; \frac{2\pi^{\frac{3}{2}}\nu!}{\Gamma(\nu + l + \frac{3}{2})} \tag{5}$$

and $S_{l+1/2}^{(\nu)}$ is a Sonine polynomial.

The resulting matrix equation may be represented by

$$\sum_{\nu' l' m'} M_{\nu lm,\nu' l' m'} F(\nu' l' m' \,|\, s\lambda\mu) \;=\; X(\nu lm \,|\, s\lambda\mu) \tag{6}$$

$$\nu, l = 0, 1, 2, ..., \infty, \qquad m = -l, \; ..., \; +l.$$

Here the matrix M consists of three distinct components, the collision term, the electric field term and the magnetic field term. Each value of the spatial indices $s\lambda\mu$ gives a set of equations, while the velocity indices νlm specify individual equations of that set. For a given value of s the X vector on the right side of (6) is given in terms of lower s values of the $F(\nu lm \,|\, s\lambda\mu)$. For practical solution, the summations in expansions (2) and (3) must be truncated. The truncation values of the indices l, m and ν are denoted by l_{max}, m_{max} and ν_{max} respectively. In the present approach l_{max}, m_{max} and ν_{max} are chosen independently. Of course m_{max} cannot exceed l_{max}, but apart from that no other restrictions are placed on the indices.

For a given value of $s\lambda\mu$ equation (6) is solved for the quantities or 'moments' $F(\nu lm \,|\, s\lambda\mu)$, which depend upon the gas temperature and mass, the interaction cross sections, and the reduced fields E/n_0 and B/n_0, where n_0 is the gas density. Having obtained the $F(\nu lm \,|\, s\lambda\mu)$, the transport coefficients and distributions functions may be calculated. For perpendicular fields with $\boldsymbol{E}$ along the z axis and $\boldsymbol{B}$ along the y axis the drift velocity and diffusion tensor are given by

$$\boldsymbol{W} = (-W_x, 0, -W_z)\,,$$

$$\mathbf{D} = \begin{bmatrix} D_x & 0 & D_{xz} \\ 0 & D_y & 0 \\ D_{zx} & 0 & D_z \end{bmatrix},$$

where W_x and W_z denote the $\boldsymbol{E}\times\boldsymbol{B}$ and $\boldsymbol{E}$ components of the drift velocity, respectively, D_x denotes the diffusion coefficient along $\boldsymbol{E}\times\boldsymbol{B}$, D_y denotes the diffusion coefficient along $\boldsymbol{B}$, D_z denotes the diffusion coefficient along $\boldsymbol{E}$, and D_{xz} and D_{zx} are the off-diagonal diffusion coefficients. The off-diagonal diffusion coefficients are reported as the sum $D_h = D_{xz} + D_{zx}$, which appears in the continuity equation. In the absence of a magnetic field, $W_x = D_{xz} = D_{zx} = 0$, and $W_z = W$, $D_x = D_y = D_T$, $D_z = D_L$. The Lorentz or magnetic deflection angle α, is defined to be the inverse of the tangent of the ratio W_x/W_z, and the net drift speed of the swarm is $W = (W_x^2 + W_z^2)^{\frac{1}{2}}$. Explicit expressions for the transport coefficients in terms of the moments are given in Ness (1994).

The spatially homogeneous velocity distribution function is obtained from the solution of the first member ($s = \lambda = \mu = 0$) of the hierarchy in equation (6) and is given by

$$f^{(0)}(\boldsymbol{c}) = f^{(0)}(c, \theta, \phi) = \sum_{l} \sum_{m=0}^{l} (-)^m F_{lm}(c)(2 - \delta_{m0}) P_l^m(\cos\theta)\cos(m\phi), \tag{7}$$

where

$$F_{lm}(c) = i^l \left[\frac{(2l+1)(l-m)!}{4\pi(l+m)!} \right]^{\frac{1}{2}} \bar{w}(\alpha, c) \sum_{\nu} F(\nu l m \,|\, 000) R_{\nu l}(\alpha c) \tag{8}$$

and P_l^m are the associated Legendre polynomials. In the absence of a magnetic field $f^{(0)}(\boldsymbol{c})$ is independent of ϕ (and therefore m) and the above equations reduce to

$$f^{(0)}(\boldsymbol{c}) = f^{(0)}(c, \theta) = \sum_l F_l(c) P_l(\cos\theta)\,, \tag{9}$$

$$F_l(c) = i^l \left[\frac{(2l+1)}{4\pi} \right]^{\frac{1}{2}} \bar{w}(\alpha, c) \sum_{\nu} F(\nu l \,|\, 00) R_{\nu l}(\alpha c). \tag{10}$$

Calculations of transport coefficients for electron swarms in both model and real gases in crossed fields have been presented elsewhere (Schmidt 1993; Ness 1994). In the present work we are interested in investigating the effects of the crossed magnetic field on the velocity distribution function of the electrons.

3. Results and Discussion

Electron transport in methane provides a good application for the calculation of electron velocity distributions functions, particularly for energies in the vicinity of the minimum in the elastic cross section where significant anisotropy in velocity space occurs. For the electron–methane cross sections we use the set by Schmidt (1991) and set the gas temperature T_0 to 295 K.

In Fig. 1 contours of constant $f^{(0)}$ are shown as a function of $\epsilon = mc^2/2$ in eV and θ in degrees for $E/n_0 = 5$ Td and $B/n_0 = 0$. In this case $f^{(0)}$ is independent of ϕ and Fig. 1 represents the intersection of any plane in velocity space passing through the origin perpendicular to the xy plane with surfaces or shells of constant $f^{(0)}$. In general the plane of intersection is specified by ϕ and $\phi + \pi$, and in this particular case ϕ may have any value. Fig. 1 clearly shows the anisotropy in velocity space by both a displacement and an elongation of the contours in the $-z$ direction. Isotropy in velocity space is represented by circular contours centred at the origin. The convergence of the transport coefficients in the l index corresponding to Fig. 1 is shown in Table 1.

The convergence of the transport coefficients in the l index reflects the anisotropy in velocity space shown in Fig. 1, where for the $f^{(0)} = 2\ (\text{eV})^{-3/2}$ contour the effect of truncation at $l = 1$ is shown by the dash–dot contour. Note the large difference in the shape of the two $f^{(0)} = 2\ (\text{eV})^{-3/2}$ contours. The contour resulting from the $l = 1$ truncation shows a significant displacement towards the $-z$ direction, but not the elongation of the multi-term result. In fact, the contour resulting from the $l = 1$ truncation shows a compression in the $-z$ direction. Both the mean energy $\bar{\epsilon}$ and the drift velocity W may be calculated from $f^{(0)}(\boldsymbol{c})$. Table 1 shows that the $l = 1$ truncation over-estimates the value of $\bar{\epsilon}$ and W by 3% and 6%, respectively, despite the large differences in the shape of the contours of $f^{(0)}$ in velocity space.

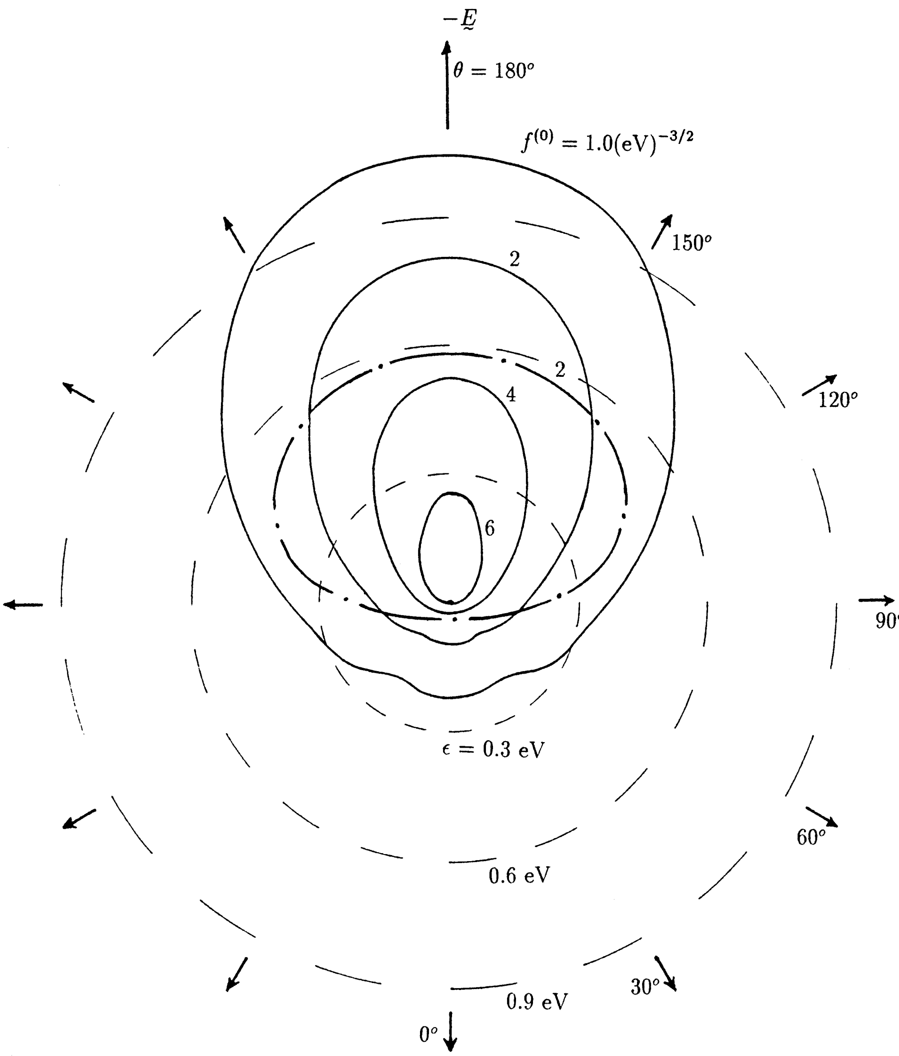

Fig. 1. Contours of constant $f^{(0)}(\boldsymbol{c})$ in units of $(\mathrm{eV})^{-3/2}$ for electrons in methane (solid curves) at $T_0 = 295$ K, $E/n_0 = 5\cdot0$ Td and $B/n_0 = 0$. The angle θ is marked in increments of 30° from 0° to 180° and three energy contours, 0·3, 0·6 and 0·9 eV are shown (thin dashed curves). The dash–dot curve gives the $f^{(0)} = 2\ (\mathrm{eV})^{-3/2}$ contour in the $l = 1$ approximation. The $-\boldsymbol{E}$ direction is indicated.

This appears to indicate that it is the displacement of $f^{(0)}$ rather than the actual shape that has the larger impact upon transport.

The effects on $f^{(0)}$ of including a perpendicular magnetic field is shown in Figs 2–4, where contours of constant $f^{(0)}$ are shown as functions of ϵ and θ for fixed values of ϕ at $E/n_0 = 5\cdot0$ Td and $B/n_0 = 30\cdot0$ Hx. The unit Hx has been defined earlier (Schmidt 1993; Ness 1994) and is given by 1 Hx $\equiv$ 1 Huxley $\equiv 10^{-27}\ \mathrm{T\,m}^3$. In Fig. 2, we have $\phi = 0,\ \pi$, i.e. we are looking at the xz plane intersection of the swarm in velocity space. The contours of $f^{(0)}$ are clearly rotated towards the $\boldsymbol{E}\times\boldsymbol{B}$

Table 1. Convergence in the l index of electron transport coefficients in methane at $E/n_0 = 5\cdot0$ Td, $B/n_0 = 0$ and $T_0 = 295$ K

l	$\bar{\epsilon}$ (eV)	W (10^4 m s^{-1})	$n_0 D_T$ (10^{24} m^{-1} s^{-1})	$n_0 D_L$ (10^{24}m^{-1} s^{-1})
1	0·619	10·6	10·6	1·87
2	0·599	9·89	6·57	2·18
3	0·602	10·0	7·44	2·02
4	0·602	10·0	7·28	2·05
5	0·602	10·0	7·30	2·05
6	0·602	10·0	7·30	2·05

directions (the $-x$ axis). Both the $-\boldsymbol{E}$ and the $\boldsymbol{E}\times\boldsymbol{B}$ directions are indicated. The elongation now occurs approximately in the direction of the Lorentz angle as indicated ($\alpha = 49\cdot7°$ from the $-z$ axis). In Fig. 3, we have $\phi = \pi/4, 3\pi/4$, while in Fig. 4, $\phi = \pi/2, 3\pi/2$. In Fig. 4 we are looking at the yz plane intersection of the swarm in velocity space; the direction of $\boldsymbol{B}$ is marked. In going from Fig. 2 to Fig. 4, observe that the contours rotate back towards the $-z$ axis and become more symmetric in velocity space. Thus in three-dimensional velocity space we have the picture of a swarm being 'drawn' in the direction of the Lorentz angle, which lies in the xz plane ($\phi = 0, \pi$). The transport coefficients corresponding to the situation in Figs 2–4 are shown in Table 2. Note that with the application of the magnetic field the mean energy of the swarm decreases from 0·602 to 0·399 eV. This is reflected in the contour plots of $f^{(0)}$ by the fact that the contours of $f^{(0)}$ in the $\boldsymbol{E}\times\boldsymbol{B}$ case are not spread out as much in velocity space as the contours for the $\boldsymbol{E}$-only case.

In one sense the magnetic field opposes the electric field, as can be seen by the reduction in the mean energy when the magnetic field is applied. This was discussed in some detail in Ness (1994), where it was also pointed out that in the limit of strong B, W_x, W_z, D_x, D_z and D_h approach zero while $\bar{\epsilon}$ and D_y approach their thermal values. This fact may also be seen in the above contours plots; besides the obvious rotation towards the $\boldsymbol{E}\times\boldsymbol{B}$ direction, there is a distinct reduction in the elongation and a general reduction in the asymmetry in velocity space when B is applied. This occurs despite the fact that electrons at 0·399 eV are more sensitive to the minimum in the electron–methane cross section than those at 0·602 eV. Thus, although the introduction of the magnetic field complicates matters by destroying the symmetry in velocity space about the electric field, an increasing magnetic field will tend to decrease the l dependence and ultimately reestablish isotropy in velocity space. In Fig. 2, the value of ϕ which shows most clearly the sensitivity of $f^{(0)}$ to both E and B, the $f^{(0)} = 1\ (\text{eV})^{-3/2}$ contour, is shown for $E/n_0 = 5\cdot0$ Td and $B/n_0 = 300\cdot0$ Hx by the dash–dot contour. For these values of the fields we have $\alpha = 85\cdot7°$, $\bar{\epsilon} = 0\cdot0770$ eV, and the $f^{(0)} = 1\ (\text{eV})^{-3/2}$ contour shows the trend of reestablishing isotropy in velocity space for strong magnetic fields. If the magnetic field is increased by a further order of magnitude to 3000·0 Hx the mean energy falls to 0·0575 eV, $\alpha = 89\cdot4°$, and the $f^{(0)} = 1\ (\text{eV})^{-3/2}$ contour is almost a circle of radius 0·16 eV, centred at the origin in velocity space. In this case the $l = 1$ approximation agrees to four significant figures with the converged multi-term result, for both

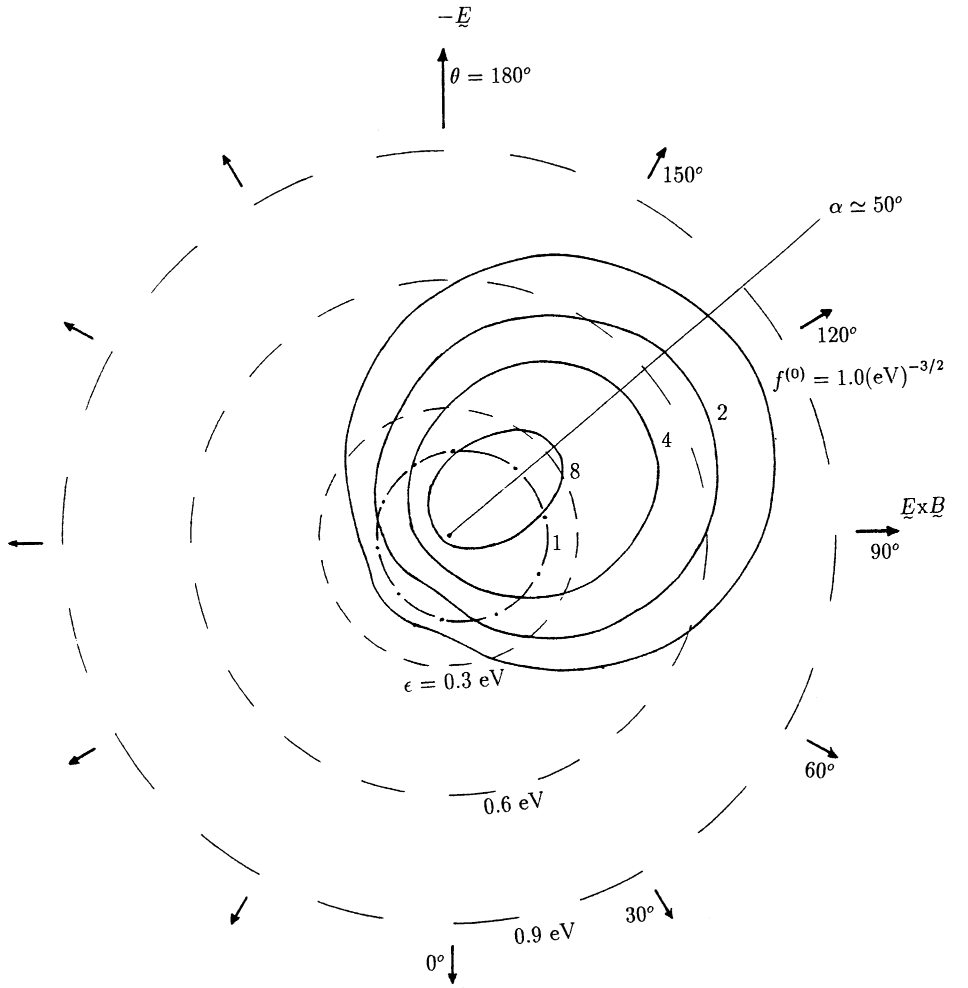

Fig. 2. Contours of constant $f^{(0)}(\boldsymbol{c})$ in units of $(\mathrm{eV})^{-3/2}$ for electons in methane (solid curves) at $T_0 = 295$ K, $E/n_0 = 5\cdot0$ Td and $B/n_0 = 30\cdot0$ Hx for $\phi = 0, \pi$. The Lorentz angle is $\alpha \approx 50^\circ$ and is indicated by the thin line drawn from the origin. The dash–dot curve is the $f^{(0)} = 1$ $(\mathrm{eV})^{-3/2}$ contour when B/n_0 is increased to $300\cdot0$ Hx while E/n_0 is held fixed. The $-E$ and the $E\times B$ directions are indicated.

drift and diffusion coefficients. It is also useful to compare distribution functions for different field strengths, but the same mean energy. By keeping the mean energy the same it is hoped that any differences in $f^{(0)}$ will be due to the different fields and not the dependence upon the cross sections. This of course will not be strictly true, as the dependence upon the cross sections will vary with the actual energy dependence of the distribution and not simply with the average energy $\bar{\epsilon}$. In Fig. 5 contours of $f^{(0)}(\boldsymbol{c})$ are shown for $E/n_0 = 3\cdot4$ Td and $B/n_0 = 0$. In this case $\bar{\epsilon} = 0\cdot399$ eV, the same value to three significant figures as for $E/n_0 = 5\cdot0$ Td and $B/n_0 = 30\cdot0$ Hx. Comparing Fig. 5 with Figs 2–4, we see that the elongation of the contours is more pronounced for the E-only case. The contours

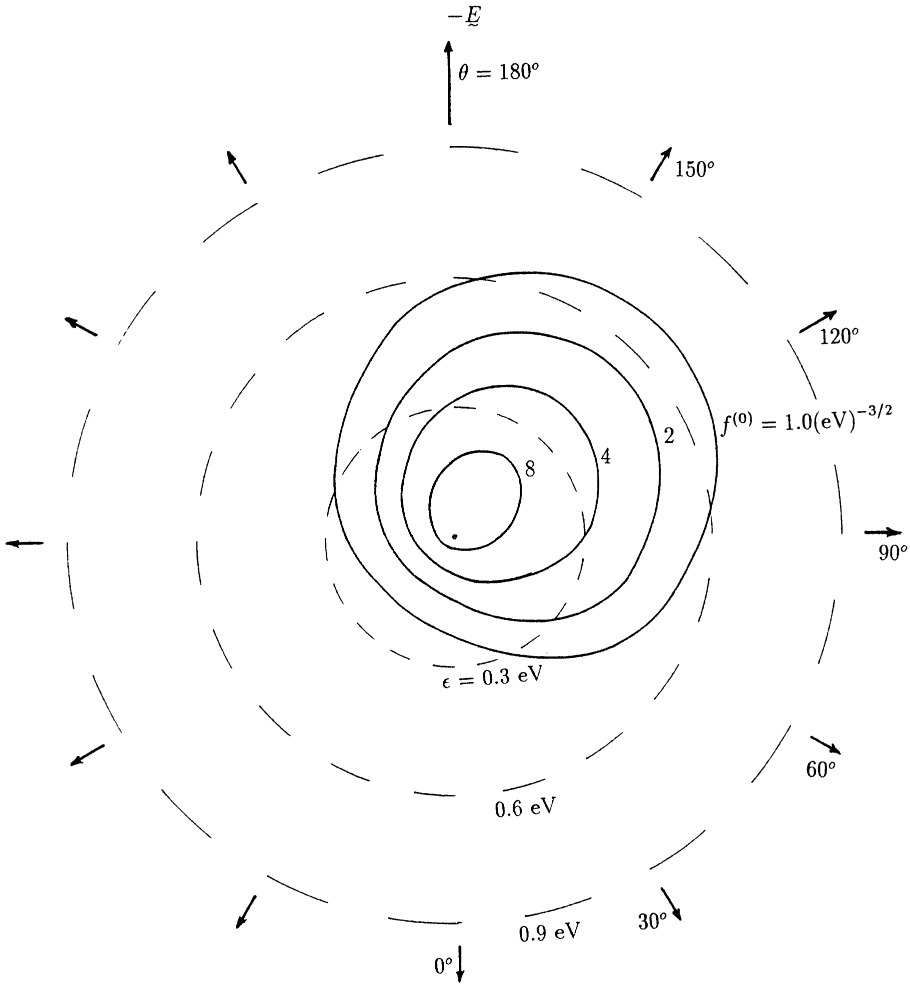

Fig. 3. Contours of constant $f^{(0)}(c)$ in units of $(\text{eV})^{-3/2}$ for electrons in methane (solid curves) at $T_0 = 295$ K, $E/n_0 = 5\cdot0$ Td and $B/n_0 = 30\cdot0$ Hx for $\phi = \pi/4$, $3\pi/4$.

in Fig. 5 are essentially a cooler version of those in Fig. 1. The transport coefficients corresponding to the conditions of Fig. 5 are shown in Table 3. The error in the $l = 1$ truncation of both $\bar{\epsilon}$ and W is a little larger for $E/n_0 = 3\cdot4$ Td than for $E/n_0 = 5\cdot0$ Td; $3\cdot3\%$ compared to $2\cdot8\%$ for $\bar{\epsilon}$ and $7\cdot5\%$ compared to 6% for W, respectively. The error in the $l = 1$ truncation of the diffusion coefficients is also larger for the weaker electric field. The elastic electron–methane cross section has a deep minimum near $0\cdot3$ eV, and this decrease in the accuracy of the $l = 1$ truncation arises because of the rapid decrease in the electron–methane elastic cross section when the swarm is cooled from $0\cdot602$ eV at $E/n_0 = 5\cdot0$ Td to $0\cdot399$ eV at $E/n_0 = 3\cdot4$ Td. Thus, on the basis of the l convergence of the transport coefficients in Tables 1 and 3, one may conclude that the swarm at $3\cdot4$ Td is more anisotropic in velocity space than the swarm at $5\cdot0$ Td, but this detail is not evident from the contour plots in Figs 1 and 5.

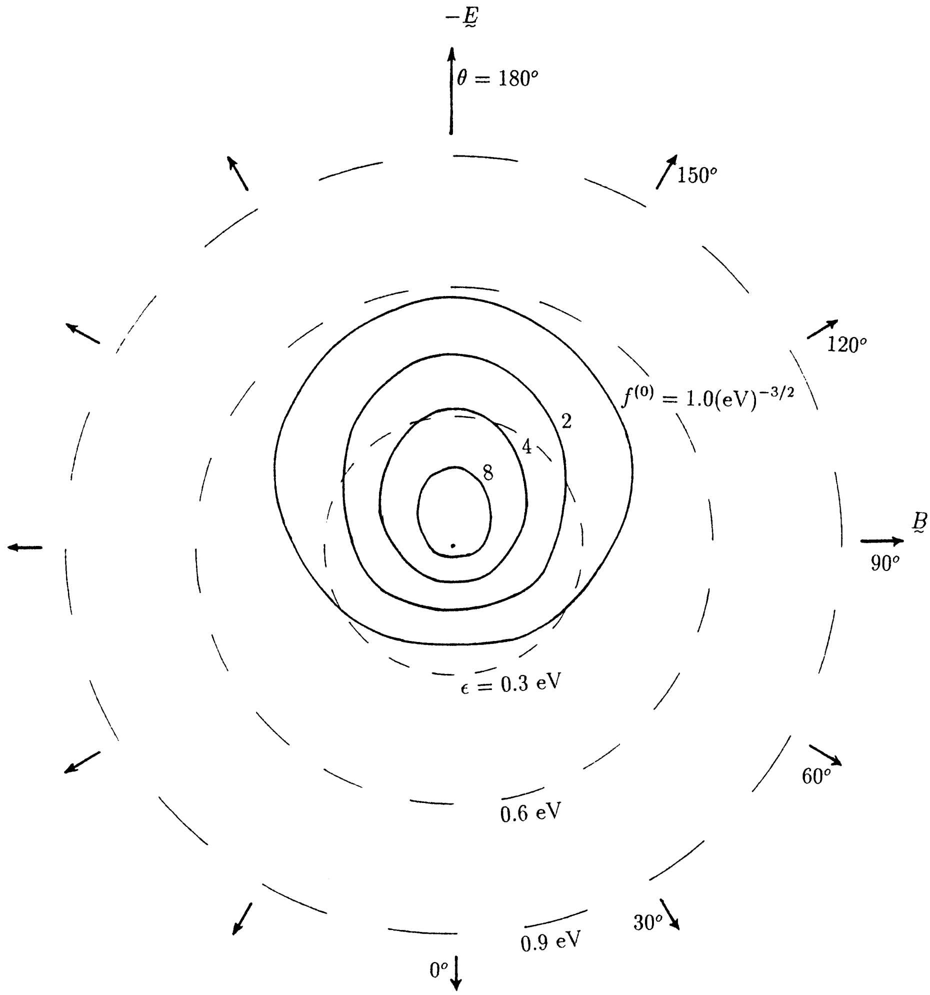

Fig. 4. Contours of constant $f^{(0)}(c)$ in units of $(\text{eV})^{-3/2}$ for electrons in methane (solid curves) at $T_0 = 295$ K, $E/n_0 = 5\cdot0$ Td and $B/n_0 = 30\cdot0$ Hx for $\phi = \pi/2, 3\pi/2$. The $-\boldsymbol{E}$ and the $\boldsymbol{B}$ directions are indicated.

Table 2. Convergence in the l index of electron transport coefficients in methane at $E/n_0 = 5\cdot0$ Td, $B/n_0 = 30\cdot0$ Hx, $T_0 = 295$ K and $m_{max} = 4$

l	$\bar{\epsilon}$ (eV)	W_x	W_z (10^4 m s^{-1})	W	n_0D_x	n_0D_y (10^{24} m^{-1} s^{-1})	n_0D_z	n_0D_h
1	0·377	8·63	6·27	10·7	4·66	9·27	2·51	3·97
2	0·396	8·26	6·84	10·7	6·44	6·90	2·20	3·66
3	0·399	8·19	6·91	10·7	6·33	6·98	2·13	3·44
4	0·399	8·19	6·92	10·7	6·30	7·02	2·12	3·40
5	0·399	8·19	6·92	10·7	6·31	7·04	2·12	3·40
6	0·399	8·19	6·92	10·7	6·31	7·04	2·12	3·40

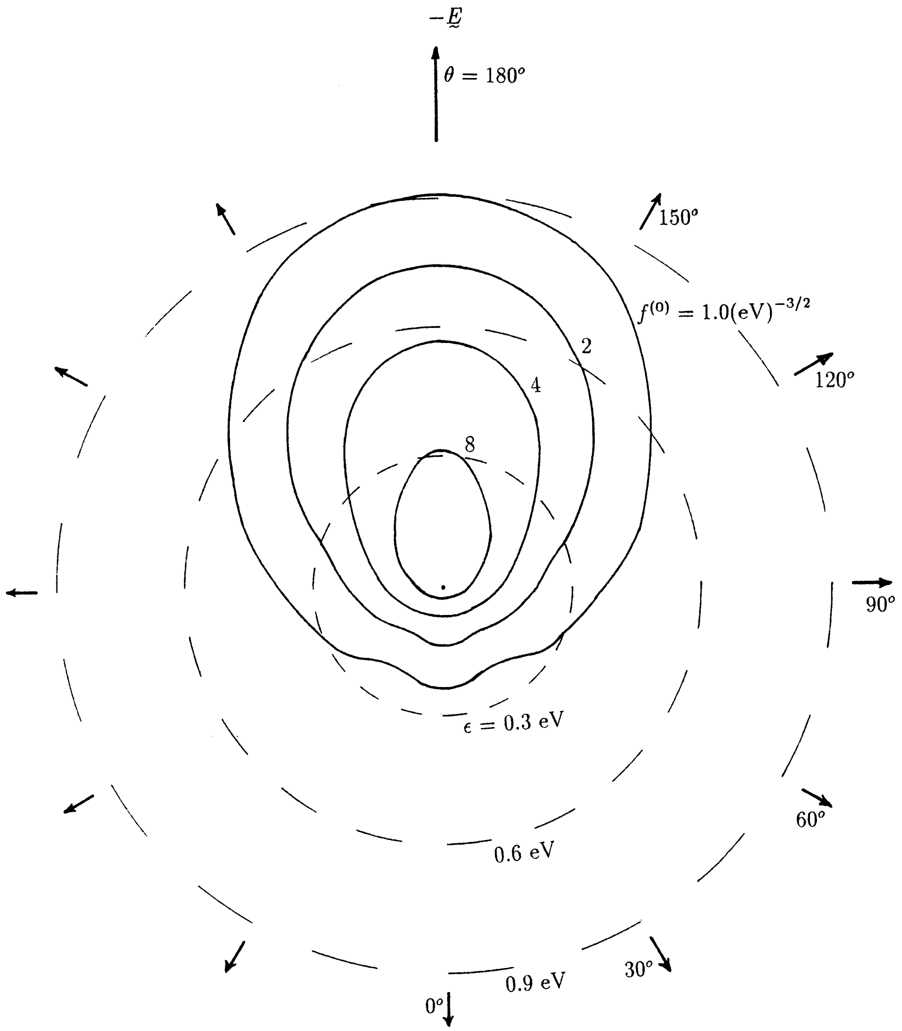

Fig. 5. Contours of constant $f^{(0)}(\boldsymbol{c})$ in units of $(\mathrm{eV})^{-3/2}$ for electrons in methane (solid curves) at $T_0 = 295$ K, $E/n_0 = 3{\cdot}4$ Td and $B/n_0 = 0$.

In Fig. 6 the $l = 0$ velocity distribution functions, calculated from equations (8) and (10), are shown as functions of electron energy for $(E/n_0,\ B/n_0) = (5{\cdot}0\ \mathrm{Td},\ 0)$, $(5{\cdot}0\ \mathrm{Td},\ 30{\cdot}0\ \mathrm{Hx})$ and $(3{\cdot}4\ \mathrm{Td},\ 0)$. These functions satisfy the normalisation condition

$$4\pi \int_0^\infty c^2 F_{00}\, dc = 1.$$

The swarm mean energy can also be calculated from these functions and is given by

$$\bar{\epsilon} = 2\pi m \int_0^\infty c^4 F_{00}\, dc.$$

Table 3. Convergence in the l index of electron transport coefficients in methane at $E/n_0 = 3 \cdot 4$ Td, $B/n_0 = 0$ and $T_0 = 295$ K

l	$\bar{\epsilon}$ (eV)	W (10^4 m s^{-1})	$n_0 D_T$ (10^{24} m^{-1} s^{-1})	$n_0 D_L$ (10^{24} m^{-1} s^{-1})
1	0·412	11·4	10·4	2·06
2	0·397	10·5	6·19	2·86
3	0·399	10·6	6·90	2·64
4	0·399	10·6	6·83	2·67
5	0·399	10·6	6·82	2·67
6	0·399	10·6	6·82	2·67

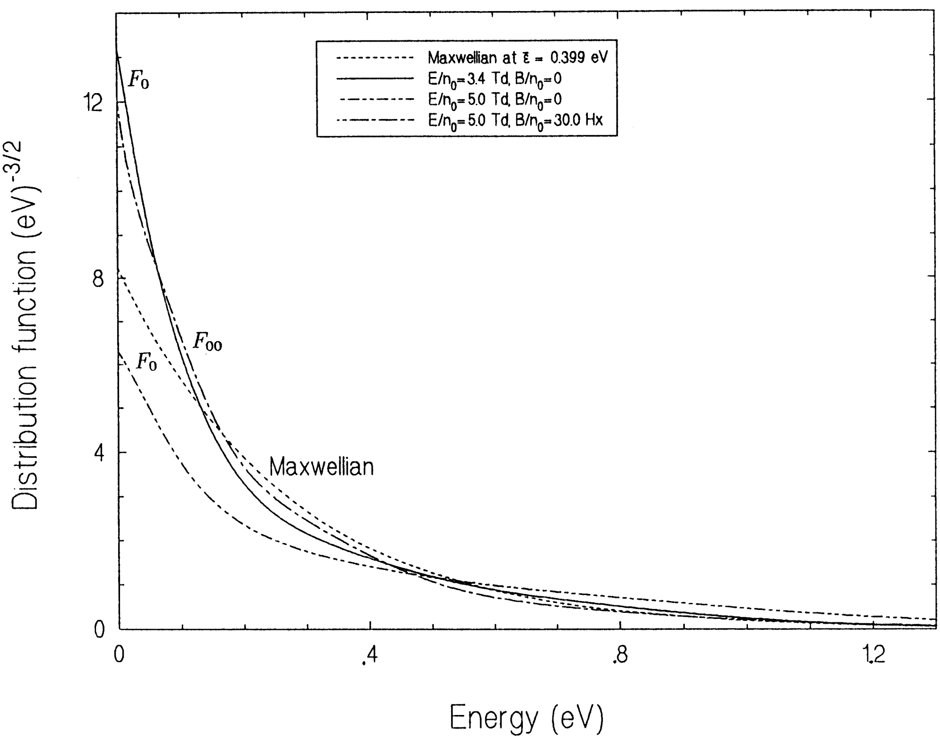

Fig. 6. Velocity distributions functions F_0 and F_{00} for electrons in methane for the three combinations of E/n_0 and B/n_0 indicated. The Maxwellian velocity distribution function with $\bar{\epsilon} = 0 \cdot 399$ eV is also shown.

The function F_{00} or F_0 results from the integration of $f^{(0)}(\boldsymbol{c})$ over the angles in velocity space, and they reflect the above contour plots. The largest value of $\bar{\epsilon}$ occurs at $E/n_0 = 5 \cdot 0$ Td, $B/n_0 = 0$, and the corresponding function F_0 in Fig. 6 has the smallest maximum and the thickest tail, indicating a greater spread in velocity space as observed in the contour plots. The functions F_{00} and F_0 corresponding to $E/n_0 = 5 \cdot 0$ Td, $B/n_0 = 30 \cdot 0$ Hx and to $E/n_0 = 3 \cdot 4$ Td, $B/n_0 = 0$, respectively, give the same mean energy. For comparison, the Maxwellian distribution at the same mean energy, $\bar{\epsilon} = 0 \cdot 399$ eV, has also been plotted in Fig. 6. Both F_0 and F_{00} are significantly different from the Maxwellian

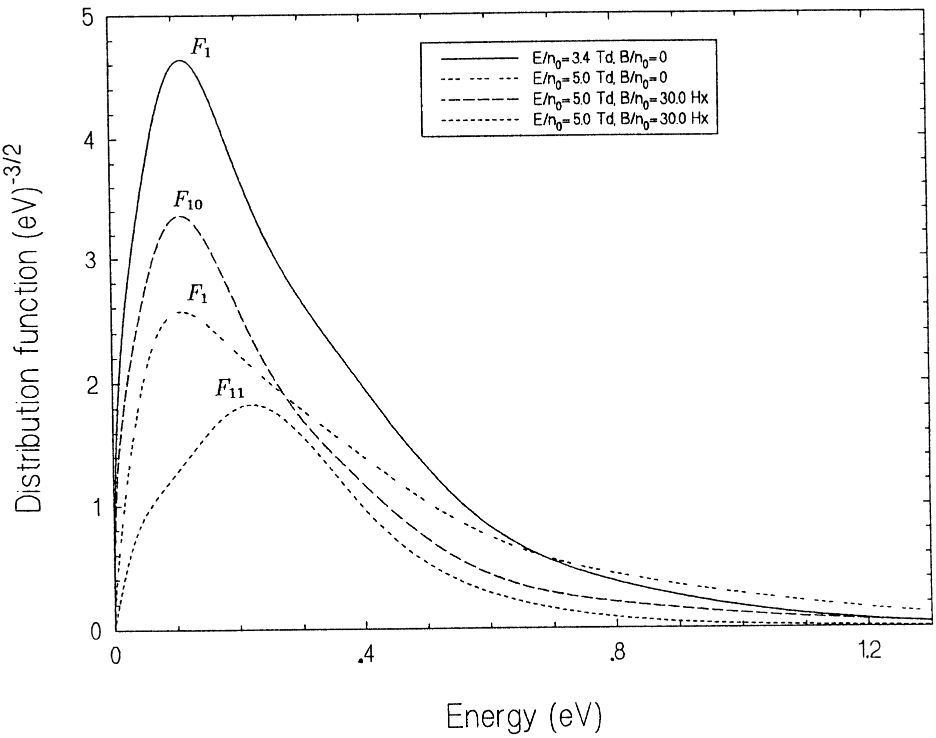

Fig. 7. Velocity distribution functions F_1, F_{10} and F_{11} for electrons in methane for the three combinations of E/n_0 and B/n_0 indicated.

at low energies. For high energies both approach the Maxwellian form, with F_{00} doing so sooner than F_0.

In Fig. 7, the $l = 1$ velocity distribution functions are plotted as functions of electron energy for the same field values as in Fig. 6. In the non-zero magnetic field case there are two functions, corresponding to $m = 0$ and $m = 1$. The drift speeds are given as integrals over these functions:

$$W_x = \frac{8\pi}{3}\int_0^\infty c^3 F_{11}\, dc \qquad W_z = \frac{4\pi}{3}\int_0^\infty c^3 F_{10}\, dc.$$

In the absence of a magnetic field we have

$$W = \frac{4\pi}{3}\int_0^\infty c^3 F_1\, dc.$$

4. Summary

The spatially homogeneous velocity distribution function for an electron swarm in methane in the presence of perpendicular electric and magnetic fields has been calculated, using a multi-term solution of the Boltzmann equation outlined in Section 2. The mean energy of the swarm was chosen to lie in the vicinity of the minimum in the elastic electron–methane cross section in order to optimise the anisotropy in velocity space. The velocity distribution function $f^{(0)}(\epsilon, \theta, \phi)$ was presented in the form of two dimensional contour plots, in polar coordinates, of constant $f^{(0)}$ as a function of ϵ and θ for a number of fixed values of ϕ. Using these plots the effect of the applied fields, in velocity space, upon the swarm was demonstrated, and a discussion of the impact of the magnetic field on the anisotropy in velocity space was given. In particular the rotation of the swarm away from the $-\boldsymbol{E}$ direction towards the $\boldsymbol{E} \times \boldsymbol{B}$ direction, when the perpendicular magnetic field is applied, was clearly shown. Transport coefficients and the $l = 0$ and the $l = 1$ spherical-harmonic components of $f^{(0)}(\epsilon, \theta, \phi)$ corresponding to the conditions of the contour plots were also presented.

Acknowledgments

The author wishes to thank Mr R. D. White in helping to prepare the manuscript.

References

Allis W. P. (1955). *In* 'The Encyclopedia of Physics' (Ed. S. Flugge), Vol. XXI, p. 383 (Springer: Berlin).
Heintze, J. (1978). *Nucl. Instrum. Meth.* **156**, 227.
Heintze, J. (1982). *Nucl. Instrum. Meth.* **196**, 293.
Heylen, A. D. E. (1980). *Proc. IEE* **127**, 221.
Huxley, L. G. H., and Crompton, R. W. (1974). 'The Diffusion and Drift of Electrons in Gases' (Wiley: New York).
Ness, K. F. (1993). *Phys. Rev.* E **47**, 327.
Ness, K. F (1994). *J. Phys.* D. **27**, 1848.
Ness, K. F., and Robson, R. E. (1994). *Phys. Scripta* **T53**, 5.
Schmidt, B. (1991). *J. Phys.* B. **24**, 4809.
Schmidt, B. (1993). *Comm. Atom. Mol. Phys.* **28**, 379.
Schmidt, B., Berkhan, K., Götz, B., and Müller, M. (1994). *Phys. Scripta* **T53** 30.

Manuscript received 23 December 1994, accepted 1 February 1995